Systemic Delivery of siRNA *via* LCP Nanoparticle Efficiently Inhibits Lung Metastasis

Yang Yang[1], Jun Li[1], Feng Liu[1] and Leaf Huang[1]

[1]*Division of Molecular Pharmaceutics, Eshelman School of Pharmacy, University of North Carolina at Chapel Hill, Chapel Hill, North Carolina, USA*

Targeted delivery remains the major challenge for the application of small interfering RNA (siRNA). We have developed a lipid/calcium/phosphate (LCP) nanoparticle (NP) to improve siRNA delivery efficiency. The LCP NP was prepared by using microemulsion technology to form calcium/phosphate (CaP) core and further coated with cationic lipids. The final NP was grafted with polyethylene glycol (PEG) and anisamide (AA) ligand on the surface to target sigma receptor-expressing B16F10 melanoma cells. The LCP NP exhibited a 40 nm particle size, a +25 mV zeta-potential, and 91% siRNA encapsulation efficiency. After a single intravenous (i.v.) injection of antiluciferase siRNA (0.12 mg siRNA/kg) formulated in targeted LCP NP, luciferase activity in metastatic B16F10 tumor-loaded lungs decreased by 78% in C57BL/6 mice. In a therapeutic experiment, siRNA against MDM2, c-myc, and VEGF coformulated in the targeted LCP NP resulted in simultaneous silencing of the respective oncogenes in metastatic nodules. Treatment with siRNA in the targeted NP significantly reduced lung metastases (~70–80%) at a relatively low dose (0.36 mg/kg), whereas control group showed little therapeutic effect. Moreover, this targeted LCP NP significantly prolonged the mean survival time of the animals by 27.8% compared to control group without showing any toxicity at the therapeutic dose.

Received 2 September 2011; accepted 14 November 2011; published online 20 December 2011. doi:10.1038/mt.2011.270

INTRODUCTION

Metastasis is a complex process requiring tumor cell detachment from the primary tumor and migration to secondary site.[1] Because of this dangerous aggressiveness, metastatic disease is a leading cause of cancer mortality. The lung, in particular, is a common site of metastasis due to its anatomic and functional structure. Moreover, the lung is highly vascular and rich in oxygen, providing not only pathways for metastatic seeding, but also a nutrient-rich environment for neoplastic growth.[2] Tumor lung metastases are found in 20–54% of deceased cancer patients.[3] Surgical resection is a widely accepted procedure for treating lung metastases. Unfortunately, due to local and distant recurrences, the reported 5-year survival rates for patients with metastatic disease are only 30–40% even after complete resection. Chemotherapy, in particular, is helpful in preventing metastasis. However, chemotherapy is often associated with serious side effects that significantly lower patients' quality of life. Thus, novel systemic treatments of tumor metastasis are urgently needed.[4,5]

RNA interference technology has stood out as one of the most attractive new antitumor therapeutics because of its revolutionary potency and selectivity for targeted gene silencing.[6] However, the practical applications of small interfering RNA (siRNA) are limited for its inherent instability against nucleases and poor bioavailability.[7] Therefore, efficient and biocompatible methods of *in vivo* siRNA delivery are needed to realize its full therapeutic potential. Recently, we have developed a novel siRNA delivery vehicle, the "lipid/calcium/phosphate" (LCP) nanoparticle (NP), by replacing the protamine/DNA core in our previous well-established LPD (liposome/polycation/DNA) formulation with a pH-sensitive calcium phosphate (CaP) core. Although the LPD formulation has shown success in delivering siRNA for metastatic lung tumor treatment, improvements were needed to address the low siRNA release efficiency and moderate toxicity.[8–12] CaP is considered as an ideal biomaterial for various biomedical applications, because it is biocompatible, biodegradable, and native to the body as the principle mineral component of teeth and bones.[13,14] Calcium ions are also known to form complexes with the nucleic acid backbone and thus may stabilize certain DNA structures.[15] Moreover, CaP can rapidly dissolve at the acidic endosome pH, releasing its cargo into the cytoplasm.[12] We have earlier shown that compared to the LPD formulation, our targeted LCP NP releases more cargo to the cytoplasm, leading to a significant (~40-fold *in vitro* and ~4-fold *in vivo*) improvement in siRNA delivery.

In the present study, we aim to investigate the feasibility of the LCP NP as a siRNA delivery vector for the treatment of metastatic tumors. Based on previous findings, we hypothesized that our LCP NP could prolong the circulation time and elevate endosome release efficiency of siRNA, lowering the required siRNA dose and the *in vivo* toxicity of the delivery system. To this end, an experimental lung metastasis model was established by the intravenous (i.v.) injection of murine melanoma cells (B16F10 cells stably transduced with the firefly luciferase gene) into C57BL/6 mice. *In vivo* gene silencing efficiency was assayed using antiluciferase siRNA formulated in targeted or nontargeted LCP NP. In order to evaluate the therapeutic efficacy of LCP NP, we chose

Correspondence: *Leaf Huang, Division of Molecular Pharmaceutics, School of Pharmacy, 1315 Kerr Hall, Chapel Hill, North Carolina 27599, USA. E-mail: leafh@unc.edu*

a combination treatment of three different siRNA sequences (MDM2/c-myc/VEGF = 1:1:1, weight ratio), which has been shown to have a synergistic antitumor effect on B16F10 tumor metastasis.[11,16]

RESULTS AND DISCUSSION

Characterization of LCP NP

CaP NPs represent a unique class of nonviral vectors, which has the potential to be an efficient, alternative siRNA delivery system. Although many studies have been performed to prepare nanosized CaP NPs to improve transfection reproducibility and efficiency, no method has produced colloidally stable particles. Typically, significant agglomeration is observed, which hampers the *in vivo* application of the CaP NP.[17–19] In the present study, we have used a newly developed CaP NP formulation, named LCP, to deliver therapeutic siRNAs in a mouse lung metastasis model of melanoma. The salient features of LCP include an asymmetrical lipid bilayer coating the CaP core that encapsulates siRNA. To enhance tumor uptake, LCP was coated with polyethylene glycol (PEG) (2 kDa) and anisamide (AA) targeting ligand for the sigma receptor overexpressing melanoma cells. The characteristics of the LCP NP are summarized in **Table 1**. The final LCP NP was ~40 nm in size, with a zeta-potential around 25 mV. The particle sizes of nontargeted and targeted NP formulations were similar to each other. The zeta-potential of the targeted NP was slightly higher than that of the nontargeted NP due to the positively charged AA ligand. Additionally, neither the nontargeted nor the targeted LCP NP formed aggregates in 50% serum (data not shown). The siRNA trapping efficiency of the LCP NP was determined to be ~91% using Texas red-labeled siRNA.

Table 1 Characterization of LCP NP formulations

	Nontargeted LCP NP	Targeted LCP NP
Particle size (nm)	40 ± 3	38 ± 5
Zeta-potential (mv)	20 ± 2	25 ± 3

Abbreviations: LCP, lipid/calcium/phosphate; NP, nanoparticle.
The particle size and zeta-potential of nontargeted and targeted LCP NP were measured using a Zetasizer. Data are representative data from repeated measures of 3–4 samples.

In vivo luciferase gene silencing

To evaluate the *in vivo* delivery efficiency of targeted LCP NP, we encapsulated luciferase siRNA and injected the targeted LCP NP into B16F10 tumor-bearing mice *via* the tail vein. The results indicated that targeted LCP NP could significantly silence luciferase expression (78%) when compared the untreated group (**Figure 1a**). Quantitative PCR also revealed that the luciferase mRNA level in the targeted LCP NP group was downregulated by 80% compared to that of control groups (**Figure 1b**). Furthermore, a dose–response assay indicated that the ED_{50} of the targeted LCP NP formulation was 60 μg/kg. The optimal dose for the maximum gene silencing effect was 120 μg/kg; further dose increases did not result in a higher luciferase silencing activity (**Figure 1c**). We have shown that our previous LPD formulation is strikingly successful for delivering siRNA after i.v. injection in the B16F10 metastasis model (ED_{50} = 75 μg/kg).[11] However, the LPD particle demonstrates variable release of siRNA into the cytoplasm among different cells. Thus, we replaced the protamine/DNA core of LPD with a pH sensitive CaP core, which could dissolve in the low pH microenvironment of the endosome, increase the osmotic pressure, and cause endosome swelling and bursting for a more consistent release of entrapped siRNA into the cytoplasm.[12] Consistent with this finding, the current study has shown that replacing the protamine/DNA core with CaP decreased the ED_{50} of the targeted NP formulation. Therefore, the enhanced activity of our present formulation is probably due to improved endosome release efficiency. Moreover, without the targeted ligand, the LCP NP only showed slight luciferase silencing, demonstrating that the targeted LCP NP can specifically bind to metastatic tumor cells and mediate ligand-induced endocytosis.

In vivo antitumor/antimetastasis study

Based on the *in vivo* luciferase gene silencing study, we next evaluated the potential of our novel LCP NP as a siRNA delivery vehicle for the treatment of tumor metastasis in the lung by encapsulating combined siRNA sequences in the LCP NP (MDM2/c-myc/VEGF = 1:1:1, weight ratio). In most cancers, the inhibition of a single gene is insufficient to suppress tumor growth. The simultaneous obstruction of several signaling pathways has been shown

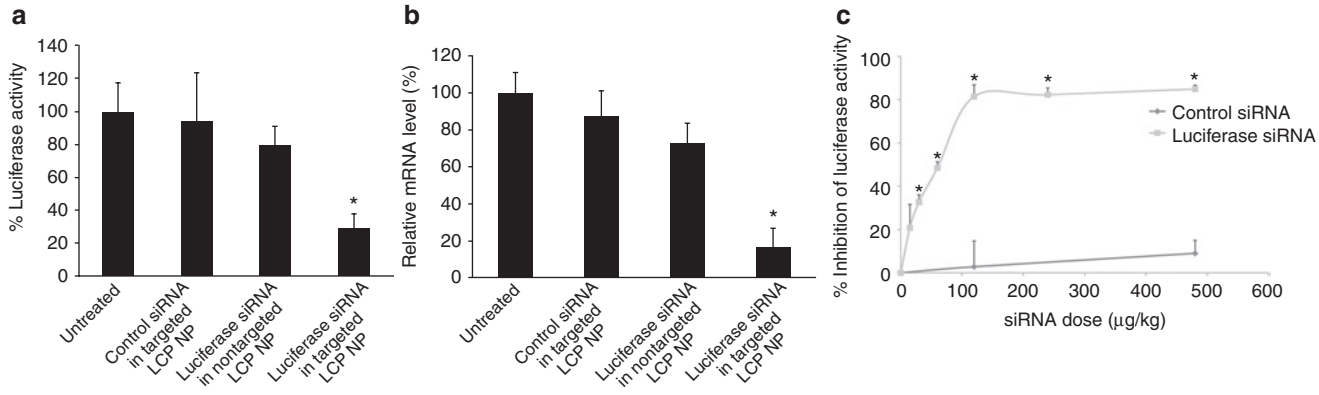

Figure 1 *In vivo* **luciferase gene silencing effect of lucifersase small interfering RNA (siRNA) in lipid/calcium/phosphate (LCP) nanoparticle (NP).** (**a**) Luciferase activity in each group. The luciferase activity was compared to the untreated control and expressed as % luciferase activity. (**b**) mRNA level of luciferase in each group was determined by quantitative reverse trancriptase (qRT)-PCR. (**c**) Dose–response curve of luciferase siRNA formulated in targeted LCP NP. Data = mean ± SD (n = 5). *P < 0.05.

to result in an enhanced therapeutic effect.[20,21] MDM2 is an integral part of one such destructive pathway, acting as a crucial negative regulator of p53 and the major suppressor of p53 function in tumors with aberrant MDM2 expression.[22] In addition, the activated c-myc transcription factor controls a broad spectrum of functions including proliferation and cell cycle, differentiation, sensitization to apoptotic stimuli, and genetic instability.[23] Tumors can also secrete VEGF growth factor to mediate tumor angiogenesis and metastasis.[24] In this study, we formulated three combination siRNAs (0.36 mg/kg, MDM2/c-myc/VEGF = 1:1:1, weight ratio) in targeted LCP NP and treated tumor-bearing mice on day 6, 8, 10, and 12 with i.v. injections to evaluate the therapeutic outcomes. As shown in **Figure 2a**, metastatic nodules were significantly reduced in lungs from mice treated with four systemic injections of siRNA formulated in the targeted LCP NP, whereas control siRNA formulated in targeted LCP NP had little therapeutic effect. Hematoxylin and eosin (H&E) staining also showed that lungs treated with combinations of siRNA in the targeted LCP NP contained only a few small nodules; most of the lung was free of tumor. In contrast, metastasis nodules occupied most of the lung tissue from control groups (**Figure 2b**).

To further quantify the B16F10 nodules in the lung, one lobe of the excised lung was homogenized and assayed for luciferase activity. As shown in **Figure 2c**, therapeutic siRNA in the targeted NP significantly reduced the tumor load to 20–30% as compared to the tumor load of the untreated control ($P < 0.01$). The therapeutic outcome was also analyzed in terms of animal survival (**Figure 2d**). On day 25, the survival rates for untreated controls, therapeutic siRNA in the targeted LCP NP, and control siRNA in the targeted LCP NP were 0, 0, 40, and 100%, respectively (**Figure 2d**), and the mean survival times were 22.3, 23.2, 25.1, and 28.5 days, respectively. Therapeutic siRNA in targeted and nontargeted LCP NP significantly improved animal survival compared to an untreated group ($P < 0.001$). Control siRNA in the targeted NP did not improve animal survival compared to untreated group ($P > 0.05$). Although siRNA in nontargeted did not reduce the tumor burden, animal longevity was improved significantly compared to control groups. The results suggested that multiple dosing might compensate for the relatively poor uptake efficiency of the nontargeted NP. Even though the results were statistically significant, nontargeted NP showed only moderate increases in animal lifespan. Targeted LCP NP, on the other hand, demonstrated much higher uptake and release efficiency for lung metastasis tumor cells and not only significantly reduced the tumor load in the lung (**Figure 2a–c**), but also prolonged survival by ~27.8% (**Figure 2d**).

In vivo antitumor/antimetastasis mechanism

To elucidate the mechanism underlining the antitumor/antimetastasis effect of the targeted LCP NP, gene silencing activity was measured using immunohistochemistry (**Figure 3a**), western blotting (**Figure 3b**) as well as enzyme-linked immunosorbent assay analysis (**Figure 3c**), respectively. As shown in **Figure 3b,c**, after two i.v. injections on days 10 and 12 (dose = 0.36 mg/kg) of therapeutic siRNA formulated in the targeted LCP NP, gene expression levels of MDM2, c-myc, and VEGF were silenced in B16F10 lung metastases, whereas other control treatments, including siRNA in nontargeted NP and control siRNA in targeted NP showed little silencing

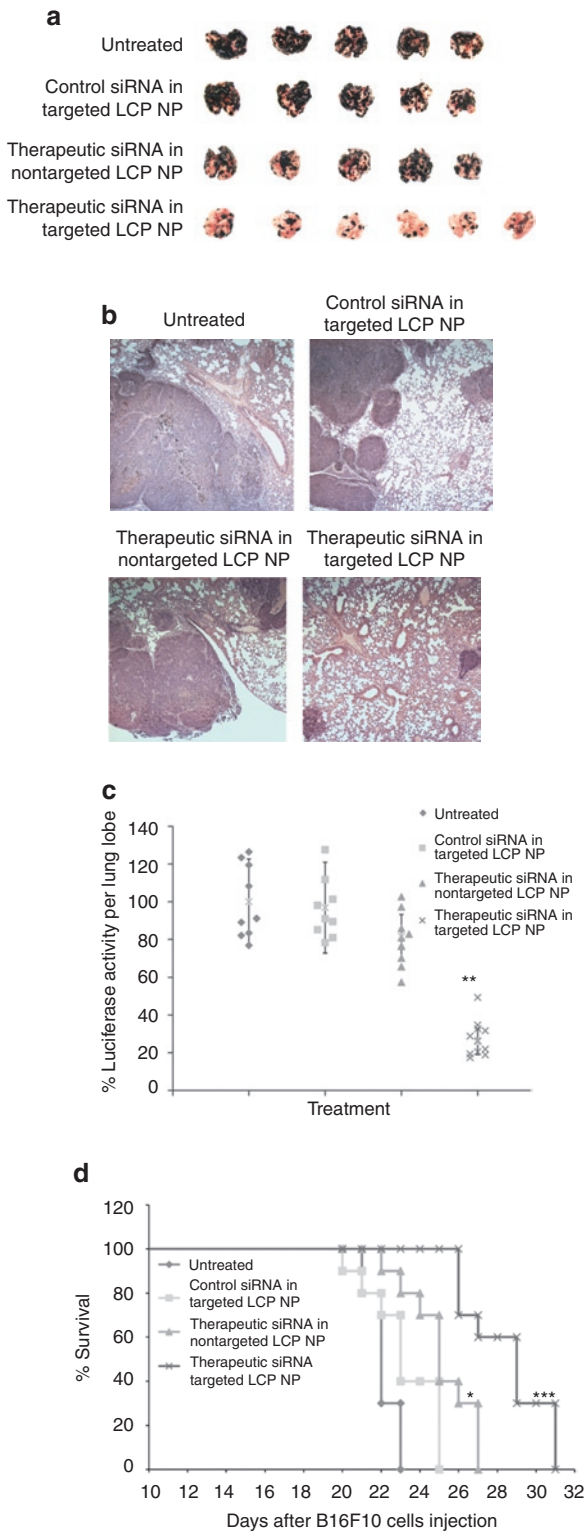

Figure 2 Antimetastasis efficacy of therapeutic small interfering RNA (siRNA) in lipid/calcium/phosphate (LCP) nanoparticle (NP). (**a**) Photographs of lungs excised from the tumor-bearing mice on day 19 after four treatments. $n = 5–6$. (**b**) Quantification of lung metastasis by measuring luciferase activity on day 19 after four injections. $n = 9–10$. (**c**) Images of hematoxylin and eosin (H&E) H&E staining of the lung tissue sections. Original magnification, ×40. (**d**) Survival analysis of B16F10 lung metastases–bearing mice after four injections. $n = 10$. $^*P < 0.05$; $^{**}P < 0.01$, $^{***}P < 0.001$.

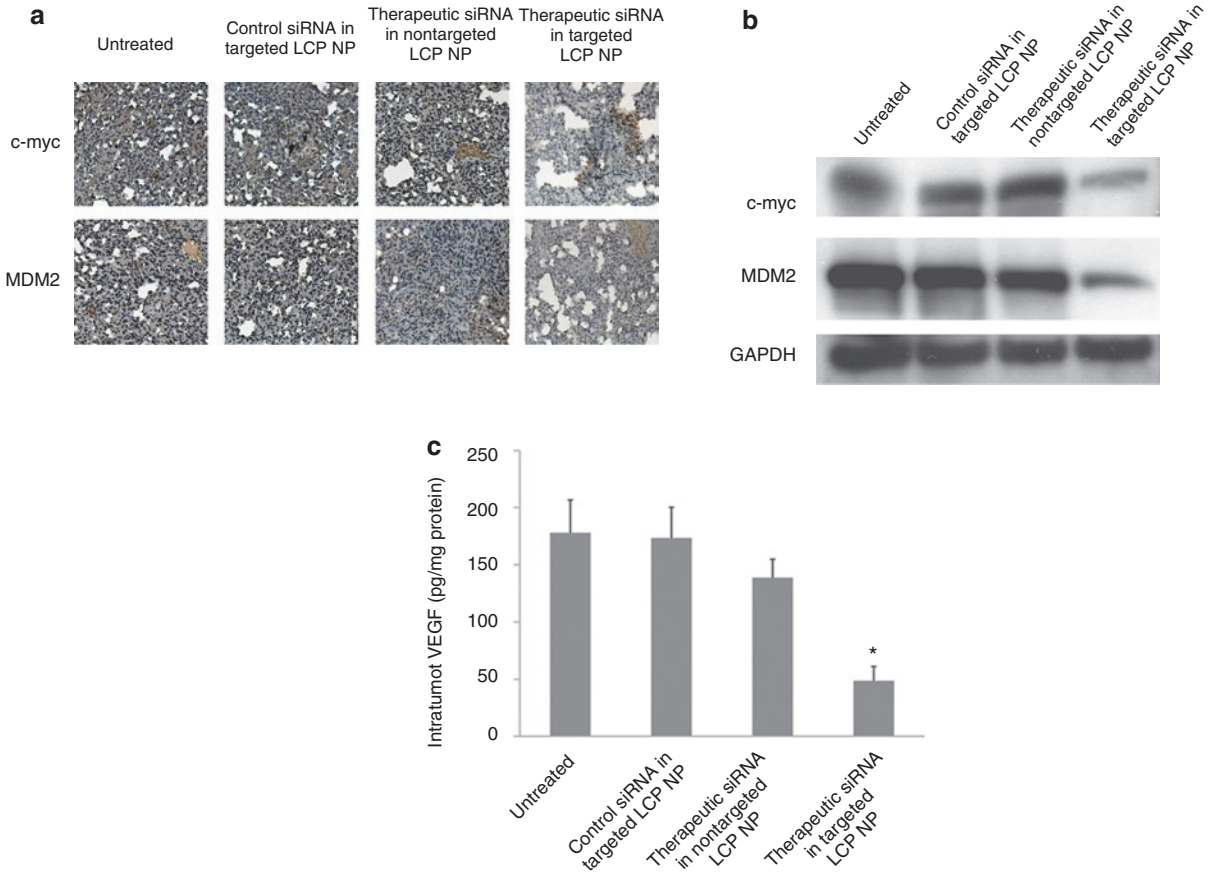

Figure 3 Oncogenes silencing in the lung metastasis. (**a**) Immunostaining of MDM2 and c-myc in the B16F10 lung metastatic nodules after two injections of **small interfering RNA (siRNA)** in different formulations. Original magnification ×100. (**b**) The protein levels MDM2 and c-myc in the B16F10 tumor-loaded lung were determined by using western blot analysis. (**c**) Intratumoral expression of VEGF after treatment with siRNA in different formulations. Data = mean ± SD (n = 5). *P < 0.05.

effect. The data from the western blotting analysis was consistent with the data obtained from the immunohistochemical analysis.

The harvested B16F10 tumors were also stained for apoptotic markers. **Figure 4** indicated that ~11% of B16F10 tumor cells treated with combination siRNA formulated in targeted NP underwent apoptosis detected by TdT-mediated dUTP Nick-End Labeling (TUNEL) staining. This value was higher than that of tumors in control groups. Moreover, we did not detect any apoptosis in the normal lung tissue area from the targeted LCP NP-treated group. Therefore, our *in vivo* results show that the antitumor/antimetastasis activity was highly dependent on the LCP NP formulation and the sequence of the encapsulated siRNA.

No immune response or major organ damage was observed after treatment with siRNA formulated in targeted LCP NP

A drug agent should not only be therapeutically effective, but must also exhibit acceptably low levels of toxicity. Recent *in vitro* reports have shown that siRNA sequences and their method of delivery might induce an interferon response.[25–27] Additionally, *in vivo* delivery of siRNA by lipids has resulted in potent interferon responses.[28,29] Here, a single tail-vein injection of the siRNA formulated in the targeted NP was performed to measure blood markers indicative of an immune response. At the therapeutic dose (0.36 mg/kg), the targeted NP did not induce significant production of any analyzed cytokines, including interleukin (IL)-6, IL-12, tumor necrosis factor, and interferon-γ at 2 or 6 hours after injection (**Figure 5a**). Furthermore, when the dose was increased twofold, inflammatory toxicity was not significantly enhanced (**Figure 5a**). Levels of secreted liver enzymes (aspartate aminotransferase and alanine aminotransferase), and blood urea nitrogen were all unchanged after a long-term treatment with therapeutic siRNA in targeted LCP NP, indicating a lack of damage to the liver or kidneys (**Table 2**). We also did a pathologic examination of the major organs (liver, kidney, spleen, heart) from the mice that received long-term treatments by H&E staining (**Figure 5b**). No organ damage was observed samples from mice treated with the formulated LCP NP. We have earlier shown that at neutral pH 7.0, both CaP and LCP NP remained unchanged.[12] Therefore, the LCP NP does not affect the serum levels of calcium and the cardiovascular physiology. Additionally, the body weight of experimental mice did not significantly decrease during treatment at the therapeutic dose (data no shown). Taken together, these results show the safety and low immunogenicity of LCP formulations and the attractiveness of this methodology for systemic, targeted delivery of nucleic acids.

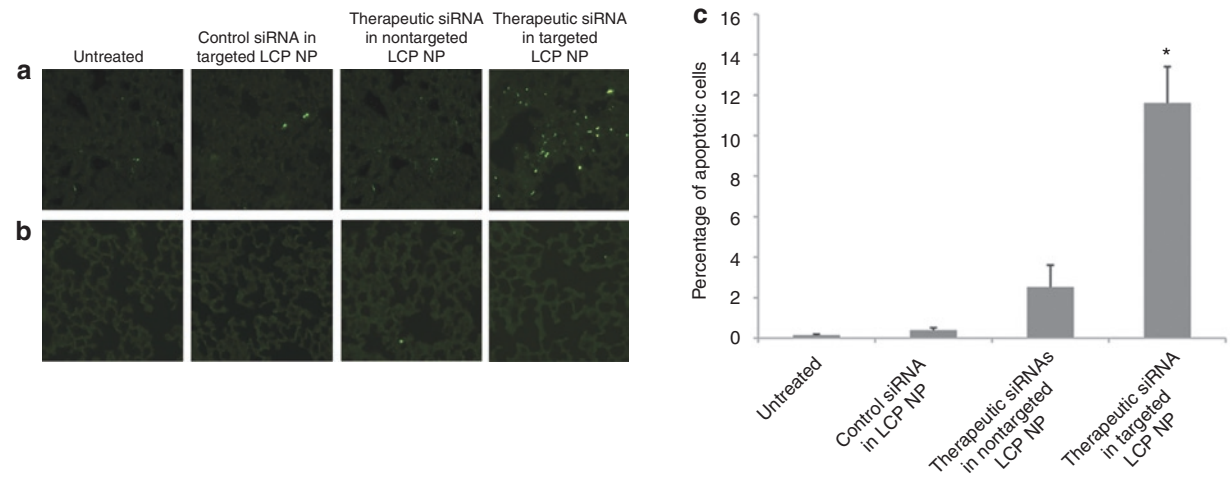

Figure 4 TdT-mediated dUTP Nick-End Labeling (TUNEL) assay. Forty-eight hours after two injections of **small interfering RNA (siRNA)** in different formulations, tumor-loaded lung were collected, sectioned and stained using a TUNEL kit. (**a**) The apoptosis was apparent in therapeutic siRNA in targeted lipid/calcium/phosphate **(LCP)** nanoparticle **(NP)**-treated tumors. (**b**) No apoptosis was observed in the normal lung area from each group. (**c**) Quantification of apoptosis in each treatment group. *$P < 0.05$ compared to the untreated group.

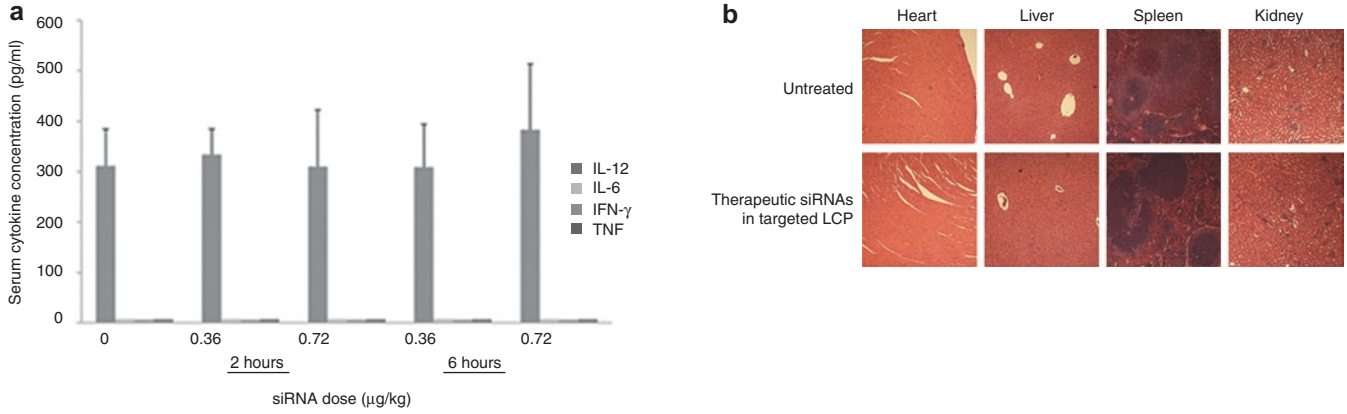

Figure 5 Toxicity analysis. (**a**) Serum cytokine assay. Serum was collected and assessed for interleukin (IL)-12, IL-6, interferon (IFN)-γ and tumor necrosis factor (TNF) at indicated time following intravenous injections of the therapeutic **small interfering RNA (siRNA)** in targeted nanoparticle at different doses. Data = mean ± SD ($n = 5$). (**b**) Hematoxylin and eosin (H&E) staining of the major organs (liver, kidney, spleen, heart) from the mice that received long-term treatments.

Table 2 Serum levels of ALT, AST and BUN after long-term treatment with therapeutic siRNA in the targeted LCP NP

	ALT (U/l)	AST (U/l)	BUN (mg/dl)
Untreated group	55.5 ± 9.12	140.5 ± 10.61	16 ± 2.83
Therapeutic siRNA in targeted LCP NP-treated group	58.33 ±17.5	149.33 ± 24.91	20 ± 5.29

Abbreviations: ALT, alanine aminotransferase; AST, aspartate aminotransferase; LCP, lipid/calcium/phosphate; NP, nanoparticle; siRNA, small interfering RNA. Measurements were carried out with the aim of evaluating the potential long-term toxicity of therapeutic siRNA in the targeted LCP NP. Data = mean ± SD ($n = 5$).

In summary, systemic delivery of siRNA by targeted LCP NP can provide safe, sequence-specific inhibition of tumor growth in a metastasis tumor model. The targeted siRNA LCP NP formulations are efficacious at low siRNA doses (0.12 mg/kg) and do not require chemical modification of the siRNA for stabilization. Furthermore, this delivery system can be easily tuned to target different cell-surface receptors in tumors and other tissue and does not elicit a detectable immune response or any changes in mouse physiology. We believe that this treatment has the potential to be developed into a useful method for inhibiting metastatic tumor growth. Future experiments using a tumor-specific targeting ligand and employing formulation combinations with small-molecule drugs are likely to further enhance the antitumoral potency of this system. We therefore conclude that siRNA formulated in targeted LCP NP has the potential to become a useful tool in cancer therapy.

MATERIALS AND METHODS

Materials. 1,2-Dioleoyl-3-trimethylammonium-propane chloride salt (DOTAP), dioleoylphosphatydic acid (DOPA), and 1,2-distearoyl-sn-glycero-3-phosphoethanolamine-N-[methoxy(polyethyleneglycol-2000)

ammonium salt (DSPE-PEG_{2000}) were purchased from Avanti Polar Lipids (Alabaster, AL). DSPE-PEG-AA (AA) was synthesized in our lab as described previously.[30] Other chemicals were obtained from Sigma-Aldrich (St Louis, MO) without further purification.

Mouse monoclonal primary antibodies against mouse MDM2, c-myc, GAPDH, and secondary antibodies conjugated with horseradish peroxidase (goat anti-mouse IgG horseradish peroxidase) were purchased from Santa Cruz Biotechnologies (Santa Cruz, CA).

Cell line. Murine melanoma cell line B16F10 cells, sigma receptor-positive, were obtained from American Type Culture Collection and stably transduced with the GL3 firefly luciferase gene using a retroviral vector in Dr Pilar Blancafort's Laboratory at the University of North Carolina at Chapel Hill. The cells were maintained in Dulbecco's modified Eagle's medium (Invitrogen, Carlsbad, CA) supplemented with 10% fetal bovine serum (Invitrogen).

Experimental animals. Female C57BL/6 mice of ages 4–6 weeks were purchased from the National Cancer Institute (Bethesda, MD). All experiments performed on the animals were in accordance with and approved by the Institutional Animal Care and Use Committee at University of North Carolina. A murine model of lung metastasis was established by intravenously injecting 2×10^5 B16F10 cells into the C57BL/6 mice.

siRNA. Luciferase siRNA (target sequence: 5′-CUU ACG CUG AGU ACU UCG A-3′), MDM2 siRNA (target sequence: 5′-GCU UCG GAA CAA GAG ACU C-3′), c-myc siRNA (target sequence: 5′-GAA CAU CAU CAU CCA GGA C-3′), VEGF siRNA (target sequence: 5′-CGA UGA AGC CCU GGA GUG C-3′), and control siRNA (target sequence: 5′-AAU UCU CCG AAC GUG UCA CGU-3′) were purchased from Dharmacon (Lafayette, CO) in unprotected, desalted, annealed form. Those sequences were adopted from published studies.[11,16]

Preparation of siRNA containing LCP NP. LCP NP was prepared as described previously with slight modifications.[12] Briefly, 600 µl of 2.5 mol/l $CaCl_2$ with 48 µg of siRNA was dispersed in a 20 ml oil phase [cyclohexane/lgepal CO-520 (71/29, vol/vol)] to form a well-dispersed water-in-oil reverse microemulsion. The phosphate microemulsion was prepared by dispersing 600 µl of 12.5 mmol/l Na_2HPO_4 (pH = 9.0) in a separate 20 ml oil phase. Two-hundred µl (20 mmol/l) DOPA in chloroform was added to the phosphate solution. After mixing the above two microemulsions for 20 minutes, 40 ml of absolute ethanol was added to the combined solution and the mixture was centrifuged at 12,000*g* for at least 15 minutes to remove the cyclohexane and surfactant. After 2–3 ethanol washes, the CaP core pellets were dissolved in 4 ml of chloroform and were stored in glass vial. To prepare the final LCP NP, 500 µl of CaP core was mixed with 75 µl of 10 mmol/l DOTAP, 10 mmol/l cholesterol, 3 mmol/l DSPE-PEG_{2000} and 3 mol/l DSPE-PEG-AA. After evaporating the chloroform, the residual lipid was hydrated in 200 µl of 5% glucose to form the LCP NP. The zeta-potential and particle size of the final LCP NP was detected in 1 mmol/l KCl by a Malvern ZetaSizer Nano series (Westborough, MA). The trapping efficiency of siRNA in LCP NP was determined as described previously using Texas Red-labeled siRNA.

In vivo *luciferase gene silencing study.* Tumor-bearing mice were given i.v. injection of antiluciferase siRNA at the dose of 0.12 mg/kg formulated in different LCP formulations. Control siRNA formulated in targeted LCP NP was also prepared to verify whether the silencing effect was sequence-dependent. For a dose–response study, tumor-bearing mice were i.v. injected with siRNA in targeted LCP NP at dose of 0.03, 0.06, 0.12, 0.24, or 0.48 mg/kg, respectively. After 24 hours, mice were sacrificed and their lungs were collected. The tumor-loaded lung was homogenized in 1 ml lysis buffer (0.05% Triton X-100 and 2 mmol/l EDTA in 0.1 mol/l–HCl) followed by centrifugation at 5,000*g* for 5 minutes. Ten µl of supernatant was mixed with 90 µl luciferase substrate (Luciferase Assay System; Promega, Madison, WI), and the luciferase activity was measured by a plate reader. The protein concentrations of the samples were determined by using BCA protein assay kit (Pierce, Rockville, MD). Luciferase activity of a sample was normalized with the protein content and expressed as percent luminescence intensity compared to the untreated control.

To determine the intratumoral level of luciferase mRNA, total RNA was extracted from the tumor-loaded lung using an RNeasy Mini Kit (Qiagen, Valencia, CA), and individual cDNAs were synthesized with a SuperScript II reverse transcriptase assay (Invitrogen). Real-time quantitative PCR was performed with a SYBR GreenER quantitative PCR SuperMix Universal kit (Invitrogen). Reactions were run with a standard cycling program; 50 °C for 2 minutes, 95 °C for 10 minutes, 40 cycles of 95 °C for 15 seconds, and 60 °C for 1 minutes, on an AB7500 real-time PCR system (Applied Biosystems, Foster City, CA). The PCR primers to detect luciferase (forward; 5′-GAA GAG ATA CGC CCT GGT TC-3′, reverse; 5′-GGC TGC GAA ATG TTC ATA CT-3′) and GAPDH (forward; 5′-ATG GGG AAG GTG AAG GTC G-3′, reverse; 5′-TAA AAG CAG CCC TGG TGA CC-3′) were synthesized and purified by IDT (Coralville, IA).

In vivo *oncogenes silencing study.* Tumor-bearing mice were given two i.v. injections of control siRNA formulated in LCP NP (0.36 mg/kg), therapeutic siRNA (MDM2/c-myc/VEGF = 1:1:1, weight ratio, 0.36 mg/kg) formulated in nontargeted LCP NP or therapeutic siRNA formulated in targeted LCP NP on days 10 and 12 after B16F10 cells inoculation. One day after the second injection, the mice were sacrificed and the tumor-loaded lungs were collected and embedded in paraffin. Immunohistological analysis of MDM2 and c-myc gene expression for extracted tissues was performed using MDM2 and c-myc monoclonal antibodies. Cell nuclei were counterstained with hematoxylin, and all the specimens were examined with a Nikon light microscope (Nikon, Tokyo, Japan). For western blotting, tumor-loaded lungs were homogenized in RIPA lysis buffer (50 mmol/l Tris, 150 mmol/l NaCl, 1% Triton, 0.5% deoxycholate, 2 mmol/l EDTA) supplemented with a 100× protease inhibitor cocktail (Sigma-Aldrich). Twenty µg of total protein extracted from the tumor-loaded lung was resolved on a sodium dodecyl sulfate polyacrylamide gel electrophoresis gel and then transferred to a polyvinylidene fluoride membrane. The membranes were blocked with 5% nonfat milk in Tris-buffered saline for 1 hour and were then incubated overnight with primary antibody at 4 °C. After five Tris-buffered saline washes (1% Tween-20 in Tris-buffered saline), the membranes were incubated with an horseradish peroxidase-conjugated secondary antibody for 1 hour. The peroxidase activity associated with the protein bands was detected with enhanced chemiluminescence using ECL plus (GE Health Care, Buckinghamshire, UK). To quantify the expression level of VEGF, the tumor-loaded lung was homogenized in phosphate-buffered saline and centrifuged at 5,000*g* for 5 minutes. Cell supernatant was collected and the concentration of VEGF was determined by using Quantikine mouse VEGF enzyme-linked immunosorbent assay kit (R&D Systems, Minneapolis, MN) according to the manufacturer's instructions. The sample concentration was calculated from the standard curve. All enzyme-linked immunosorbent assay data was corrected for total protein. Each experiment was performed in triplicate.

TUNEL assay. To detect apoptotic cells in tumor tissues, a TUNEL assay, using a DeadEndTM Fluorometric TUNEL System (Promega), was performed, following the manufacturer's protocol. Cell nuclei that were fluorescently stained dark green were defined as TUNEL-positive nuclei. TUNEL-positive nuclei were monitored by using a fluorescence microscope (Nikon, Tokyo, Japan). To quantify TUNEL-positive cells, green-fluorescence-positive cells were counted in 10 random 0.011-mm^2 fields at ×200 magnification.

In vivo *metastasis inhibition study and survival analysis.* Tumor-bearing mice were given i.v. injections of control siRNA formulated in targeted LCP NP (0.36 mg/kg), therapeutic siRNA (MDM2/c-myc/VEFG = 1:1:1, weight ratio, 0.36 mg/kg) formulated in nontargeted LCP NP or therapeutic siRNA formulated in targeted LCP NP on days 6, 8, 10, and 12. On day 19,

the mice were sacrificed and the tumor-loaded lungs were collected. One lobe of each lung was analyzed for luciferase activity in order to quantify the lung metastasis nodules. The lobe was homogenized in 1 ml of lysis buffer (0.05% Triton X-100 and 2 mmol/l EDTA in 0.1 mol/l Tris–HCl) followed by centrifugation at 5,000*g* for 5 minutes. Ten µl of the supernatant was mixed with 90 µl of luciferase substrate, and the luciferase activity was measured using a plate reader. The rest of the lung was fixed in 4% neutral paraformaldehyde solution overnight and embedded in paraffin followed by H&E staining. For the survival analysis study, tumor-bearing mice were treated on days 6, 8, 10, and 12. The mice were sacrificed if they exhibited a weight loss >10% or showed ruffled fur.

Toxicity, immune response, and pathology studies. The C57BL/6 mice were i.v. injected with siRNA (MDM2/c-myc/VEGF = 1:1:1) formulated in the targeted LCP NP at a dose of 0.36 mg/kg or 0.72 mg/kg. Two and six hours after the injection, blood samples were collected and allowed to clot for 2 hours at room temperature. Serum was obtained by centrifuging for 20 minutes at 2,000*g* and the serum cytokine level was determined using enzyme-linked immunosorbent assay kits for IL-6, IL-12, TNF-α and interferon-γ (BD Biosciences, San Diego, CA). For liver and renal function experiments, mice were i.v. injected with siRNA (MDM2/c-myc/VEGF = 1:1:1, 0.36 mg/kg) formulated in the targeted LCP NP every other day for four times. The levels of aspartate aminotransferase, alanine aminotransferase, and blood urea nitrogen in serum were measured 1 day after the last injection. Major organs of the C57BL/6 mice were collected after treatment, formalin fixed, and processed for routine H&E staining using standard methods. Images were collected using a Nikon light microscope (Nikon).

Statistical analysis. Data was presented as mean values ± SD. The statistical significance was determined using one-way ANOVA. The animal survival data was analyzed using Kaplan–Meier survival analysis. *P* values <0.05 were considered significant.

ACKNOWLEDGMENTS

We thank Michael Foote for editing the manuscript. The work was supported by NIH grants CA129835, CA149363, and CA151652. Y.Y. is on leave from the State Key Laboratory of Biotherapy, West China Hospital, Sichuan University, Sichuan The People's Republic of China.

REFERENCES

1. Mehlen, P and Puisieux, A (2006). Metastasis: a question of life or death. *Nat Rev Cancer* **6**: 449–458.
2. Zheng, Y and Fernando, HC (2010). Surgical and nonresectional therapies for pulmonary metastasis. *Surg Clin North Am* **90**: 1041–1051.
3. Hess, KR, Varadhachary, GR, Taylor, SH, Wei, W, Raber, MN, Lenzi, R *et al.* (2006). Metastatic patterns in adenocarcinoma. *Cancer* **106**: 1624–1633.
4. Krishnan, K, Khanna, C and Helman, LJ (2006). The molecular biology of pulmonary metastasis. *Thorac Surg Clin* **16**: 115–124.
5. Nguyen, DX, Bos, PD and Massagué, J (2009). Metastasis: from dissemination to organ-specific colonization. *Nat Rev Cancer* **9**: 274–284.
6. Whitehead, KA, Langer, R and Anderson, DG (2009). Knocking down barriers: advances in siRNA delivery. *Nat Rev Drug Discov* **8**: 129–138.
7. de Fougerolles, A, Vornlocher, HP, Maraganore, J and Lieberman, J (2007). Interfering with disease: a progress report on siRNA-based therapeutics. *Nat Rev Drug Discov* **6**: 443–453.
8. Li, SD and Huang, L (2006). Surface-modified LPD nanoparticles for tumor targeting. *Ann N Y Acad Sci* **1082**: 1–8.
9. Li, SD, Chen, YC, Hackett, MJ and Huang, L (2008). Tumor-targeted delivery of siRNA by self-assembled nanoparticles. *Mol Ther* **16**: 163–169.
10. Li, SD, Chono, S and Huang, L (2008). Efficient gene silencing in metastatic tumor by siRNA formulated in surface-modified nanoparticles. *J Control Release* **126**: 77–84.
11. Li, SD, Chono, S and Huang, L (2008). Efficient oncogene silencing and metastasis inhibition via systemic delivery of siRNA. *Mol Ther* **16**: 942–946.
12. Li, J, Chen, YC, Tseng, YC, Mozumdar, S and Huang, L (2010). Biodegradable calcium phosphate nanoparticle with lipid coating for systemic siRNA delivery. *J Control Release* **142**: 416–421.
13. Epple, M, Ganesan, K, Heumann, R, Klesing, J, Kovtun, A, Neumann, S *et al.* (2010). Application of calcium phosphate nanoparticles in biomedicine. *J Mater Chem* **20**: 18–23.
14. LeGeros, RZ (2008). Calcium phosphate-based osteoinductive materials. *Chem Rev* **108**: 4742–4753.
15. Cheang TY, Wang SM, Hu ZJ, Xing ZH, Chang GJ, Yao C,*et al.* (2010). Calcium carbonate/CaIP6 nanocomposite particles as gene delivery vehicles for human vascular smooth muscle cells. *J Mater Chem* **20**: 8050–8055.
16. Song, E, Zhu, P, Lee, SK, Chowdhury, D, Kussman, S, Dykxhoorn, DM *et al.* (2005). Antibody mediated *in vivo* delivery of small interfering RNAs via cell-surface receptors. *Nat Biotechnol* **23**: 709–717.
17. Zhang, M and Kataoka K (2009). Nano-structured composites based on calcium phosphate for cellular delivery of therapeutic and diagnostic agents. *Nano Today* **4**: 508–517.
18. Kakizawa, Y, Furukawa, S and Kataoka, K (2004). Block copolymer-coated calcium phosphate nanoparticles sensing intracellular environment for oligodeoxynucleotide and siRNA delivery. *J Control Release* **97**: 345–356.
19. Kakizawa, Y, Furukawa, S, Ishii, A and Kataoka, K (2006). Organic-inorganic hybrid-nanocarrier of siRNA constructing through the self-assembly of calcium phosphate and PEG-based block aniomer. *J Control Release* **111**: 368–370.
20. Gill, C, Dowling, C, O'Neill, AJ and Watson, RW (2009). Effects of cIAP-1, cIAP-2 and XIAP triple knockdown on prostate cancer cell susceptibility to apoptosis, cell survival and proliferation. *Mol Cancer* **8**: 39.
21. Addepalli, MK, Ray, KB, Kumar, B, Ramnath, RL, Chile, S and Rao, H (2010). RNAi-mediated knockdown of AURKB and EGFR shows enhanced therapeutic efficacy in prostate tumor regression. *Gene Ther* **17**: 352–359.
22. Lyubomir, TV (2007). MDM2 inhibitors for cancer therapy. *Trends Mol Med* **13**: 23–31.
23. Luoto, KR, Meng, AX, Wasylishen, AR, Zhao, H, Coackley, CL, Penn, LZ *et al.* (2010). Tumor cell kill by c-MYC depletion: role of MYC-regulated genes that control DNA double-strand break repair. *Cancer Res* **70**: 8748–8759.
24. Judah F (2002). Role of angiogenesis in tumor growth and metastasis. *Semin Oncol* **29**: 15–18.
25. Bridge, AJ, Pebernard, S, Ducraux, A, Nicoulaz, AL and Iggo, R (2003). Induction of an interferon response by RNAi vectors in mammalian cells. *Nat Genet* **34**: 263–264.
26. Sledz, CA, Holko, M, de Veer, MJ, Silverman, RH and Williams, BR (2003). Activation of the interferon system by short-interfering RNAs. *Nat Cell Biol* **5**: 834–839.
27. Hornung, V, Guenthner-Biller, M, Bourquin, C, Ablasser, A, Schlee, M, Uematsu, S *et al.* (2005). Sequence-specific potent induction of IFN-alpha by short interfering RNA in plasmacytoid dendritic cells through TLR7. *Nat Med* **11**: 263–270.
28. Judge, AD, Sood, V, Shaw, JR, Fang, D, McClintock, K and MacLachlan, I (2005). Sequence-dependent stimulation of the mammalian innate immune response by synthetic siRNA. *Nat Biotechnol* **23**: 457–462.
29. Ma, Z, Li, J, He, F, Wilson, A, Pitt, B and Li, S (2005). Cationic lipids enhance siRNA-mediated interferon response in mice. *Biochem Biophys Res Commun* **330**: 755–759.
30. Banerjee, R, Tyagi, P, Li, S, and Huang, L, (2004). Anisamide-targeted stealth liposomes: a potent carrier for targeting doxorubicin to human prostate cancer cells. *Int J Cancer* **112**: 693–700.